First- and second-order motion mechanisms are distinct at low but common at high temporal frequencies

Rémy Allard

Visual Psychophysics and Perception Laboratory, Université de Montréal, Montréal, Québec, Canada

Jocelyn Faubert

Visual Psychophysics and Perception Laboratory, Université de Montréal, Montréal, Québec, Canada

There is no consensus on the type of nonlinearity enabling motion processing of second-order stimuli. Some authors suggest that a nonlinearity specifically applied to second-order stimuli prior to motion processing (e.g., rectification process) recovers the spatial structure of the signal permitting subsequent first-order motion analyses (e.g., filter–rectify–filter model). Others suggest that nonlinearities within motion processing enable first-order-sensitive mechanisms to process second-order stimuli (e.g., gradient-based model). In the present study, we evaluated intra- and inter-attribute interactions by measuring the impact of dynamic noise modulators (either luminance (LM) or contrast-modulated (CM)) on the processing of moving LM and CM gratings. When the signal and noise were both of the same type, similar calculation efficiencies but different internal equivalent noises were observed at all temporal frequencies. At high temporal frequencies, each noise type affected both attributes by similar proportions suggesting that both attributes are processed by common mechanisms. Conversely, at low temporal frequencies, each noise type primarily impaired the processing of the attribute of the same type suggesting distinct mechanisms. We therefore conclude that two fundamentally different mechanisms are processing CM stimuli: one low-pass and distinct from the mechanisms processing LM stimuli and the other common to the mechanisms processing LM stimuli.

Keywords: second-order, contrast-modulated, motion, noise, filter–rectify–filter model, gradient-based model, feature tracking

Citation: Allard, R., & Faubert, J. (2008). First- and second-order motion mechanisms are distinct at low but common at high temporal frequencies. *Journal of Vision, 8*(2):12, 1–17, http://journalofvision.org/8/2/12/, doi:10.1167/8.2.12.

Introduction

There is no consensus on how second-order stimuli are processed. Typically, first-order stimuli are defined by luminance or color, and second-order stimuli are defined by some other attribute such as contrast, orientation, or texture (Baker, 1999; Cavanagh & Mather, 1989; Chubb & Sperling, 1988; Wilson, Ferrera, & Yo, 1992). Second-order stimuli are composed of a carrier and an envelope. The envelope locally defines a certain property of the carrier (e.g., contrast).

Some authors suggest the existence of specialized mechanisms dedicated to second-order stimuli (e.g., filter–rectify–filter model; Wilson et al., 1992), while others rather suggest that, at least for some second-order stimuli, nonlinearities within first-order-sensitive mechanisms could enable second-order perception (e.g., gradient-based model; Benton, 2002; Benton & Johnston, 2001; Benton, Johnston, McOwan, & Victor, 2001; Taub, Victor, & Conte, 1997). Luminance (LM)- and contrast-modulated (CM) patterns (Movie 1) are the more frequently used profiles to represent first- and second-order stimuli, respectively. The present paper investigated whether such motion stimuli are processed by common or separate mechanisms.

Filter–rectify–filter model

The filter–rectify–filter model suggests that LM and CM stimuli are initially processed by separated pathways (for a review, see Baker 1999). Extra processing for CM stimuli (rectification process) would reveal the spatial structure of the envelope, which could then be processed by subsequent mechanisms. Indeed, this model suggests that before perceiving the signal (i.e., envelope), the local property of the carrier should first be evaluated (in this case the contrast) followed by its variation over space (i.e., the signal or envelope). In other words, to perceive a difference of contrast, we first need to evaluate the local contrast of different spatial regions.

Gradient-based model

The fact that we can perceive second-order stimuli containing no spectral energy near the envelope frequency

doi: 10.1167/8.2.12 Received June 15, 2007; published February 28, 2008 ISSN 1534-7362

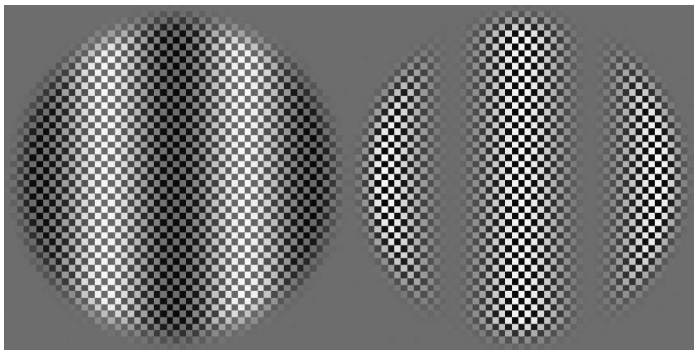

Movie 1. Luminance (left)- and contrast-modulated (right) signals drifting at a temporal frequency of 2 Hz.

led several authors to suggest the existence of a dedicated mechanism for second-order processing such as the filter–rectify–filter model presented above. However, some authors have proposed models in which both LAM and CM would be processed by common mechanisms (Benton, 2002, 2004; Benton & Johnston, 2001; Benton et al., 2001; Johnston, Benton, & McOwan, 1999; Johnston & Clifford, 1995; Johnston, McOwan, & Buxton, 1992; Taub et al., 1997). For instance, a gradient-based algorithm (Benton & Johnston, 2001) computing the temporal derivative relative to the spatial derivative could reveal the motion direction of both LAM and CM stimuli. Consequently, although CM stimuli do not have spectral energy near the envelope frequency, nonlinearities (e.g., ratio of temporal vs spatial derivatives) within motion processing could enable LM-sensitive mechanisms to also detect CM stimuli. Such an algorithm would not initially recover the spatial property of the stimulus; it would directly process the direction of motion based on the spatial and temporal local variation of luminance. One of the limits of the gradient-based model is that it would not be sensitive to all second-order stimuli (Lu & Sperling, 2001). Nonetheless, the gradient-based approach suggests that, in some conditions, the visual system may not require dedicated motion mechanisms to process second-order stimuli.

Spatial LM and CM processing

In a recent study on spatial vision (Allard & Faubert, 2007), we evaluated inter-attribute interactions between static LM and CM stimuli. We found that LM noise affected LM signal detection but had little or no impact on CM signal detection and, vice versa, CM noise affected CM signal detection but had little or no impact on LM signal detection. This double dissociation implies that both cues must be processed, at least at some point, by separate mechanisms. These results are in agreement with results showing no subthreshold summation between LM and CM stimuli (Schofield and Georgeson's, 1999) and similar detection (LM vs noise and CM vs noise) and recognition (LM vs CM) thresholds (Georgeson & Schofield, 2002), suggesting that LM and CM stimuli are processed by two separated pathways.

In another study (Allard & Faubert, 2006), we decomposed the sensitivity to static LM and CM stimuli into internal equivalent noise and calculation efficiency (Legge, Kersten, & Burgess, 1987; Pelli, 1981, 1990). The internal equivalent noise corresponds to the amount of noise added to the stimulus having the same impact as the internal noise. The calculation efficiency is inversely proportional to the smallest signal-to-noise ratio at which the signal may be detected. We found that the difference of sensitivity to LM and CM stimuli was due to a difference of internal equivalent noise and not to a difference of calculation efficiency. In other words, in high noise conditions, observers had similar detection thresholds to both LM and CM stimuli. Indeed, observers were just as efficient at detecting LM signals embedded in LM noise as CM signals embedded in CM noise. This suggests that common mechanisms could be extracting the signal from noise for both LM and CM stimuli. Schofield and Georgeson also found similar responses to static LM and CM stimuli. They observed similar spatial (Schofield & Georgeson, 1999) and temporal (Schofield & Georgeson, 2000) integration and similar sensitivity function shapes (Schofield & Georgeson, 1999). They also found inter-attribute interactions: adapting to one cue affected the perceived modulation depth of the other (Georgeson & Schofield, 2002). However, since inter-attribute adaptation effects in high contrast conditions are not very pattern selective (Ross & Speed, 1996; Snowden & Hammett, 1992, 1996), they concluded that common adaptation is not strong evidence for common processing.

Schofield and Georgeson (1999) therefore concluded that static LM and CM stimuli are processed by distinct mechanisms with similar properties that share common adaptive mechanisms. Alternatively, we proposed that the detection of static LM and CM stimuli are initially processed by separate pathways but are processed by common mechanisms at higher levels (Allard & Faubert, 2007). Based on the fact that no inter-attribute interaction was observed near threshold, we suggested that common late mechanisms could focus on either attribute without merging them. If late mechanisms were processing both attributes simply by merging them, the noise presented to one pathway would affect the detection of the signal presented to the other. We therefore suggested a gating model in which late mechanisms could select either attribute while ignoring the other.

Purpose of the present study

The main objective of the present study was to apply a similar noise-masking paradigm as the one we have used

to study static LM and CM processing in order to investigate whether LM and CM motion stimuli are processed by common or separate mechanisms. We therefore evaluated contrast thresholds of moving LM and CM signals embedded in LM and CM dynamic noise. When the signal and noise were both defined by the same attribute, it was possible to decompose the sensitivity into internal equivalent noise and calculation efficiency. Similar calculation efficiencies, i.e., similar signal-to-noise ratio required to detect the signal, would suggest that, at least at some point, both types of stimuli are processed by common mechanisms. Inter-attribute interactions were evaluated by superimposing a signal and noise defined by different attributes. No or little inter-attribute interaction would imply that both stimuli must be processed, at least at some point, by separate mechanisms. Alternatively, complete inter-attribute interactions (LM and CM noise each affecting LM and CM processing by the same proportions) would suggest that the two cues are processed by common mechanisms.

Experiment 1: Compressive nonlinearity

We are more sensitive to first-order than second-order cues. As a result, small artifacts (introduced either by the display or by the visual system) can enable first-order-sensitive mechanisms to process second-order stimuli. Experimenters must therefore assert that first-order artifacts are too small to enable, by themselves, first-order-sensitive mechanisms to process second-order stimuli.

Component motion (Scott-Samuel & Georgeson, 1999) can occur when the carrier's spectral energy is not broadband (e.g., periodic or high-pass carriers). For such carriers, the spectral energy is concentrated at some frequencies. Adding a contrast modulation to the carrier gives rise to two spectral energy peaks near each energy peak of the un-modulated carrier, which are referred to as sidebands. The sideband with the lowest spatial frequency has motion energy in the opposite direction to the CM signal, and the other has motion energy in the same direction as the CM signal. If the observer is more sensitive to the sideband with the lowest spatial frequency, then he will perceive motion in the opposite direction of the signal. In the present study, the carrier used was defined only by high spatial frequencies so component motion could have been an issue. However, the fact that a direction discrimination task was used ensures that this artifact was not a concern. Indeed, if observers were processing motion due to this artifact, then their response would have been incorrect when motion was perceived and the staircases would not have converged. Since this was not the case in all the conditions, we concluded that the results were unaffected by component motion artifacts.

When using broadband static noise as a carrier, local first-order artifacts could enable CM processing (Smith & Ledgeway, 1997). If the mean luminance of a spatial region of the carrier is not equal to the mean luminance of the entire stimulus, then adding a CM signal causes a local first-order artifact by introducing an LM signal within this region. Local first-order artifacts will be of opposite polarity for spatial regions of the carrier with lower and higher local luminance relative to the mean luminance. As a result, there will be no spectral energy in the Fourier domain since the opposite polarities will on average cancel one another. Nonetheless, there will be local direction biases at various spatial regions that could be used to discriminate the motion direction. Since the carriers used in the present study contained spectral energy only at high spatial frequencies, all local mean luminance were equal to the mean luminance of the display, and this type of artifact was therefore not an issue.

The global distortion product artifact is caused by compressive nonlinearities of the visual system (Scott-Samuel & Georgeson, 1999; Smith & Ledgeway, 1997). Indeed, it has been shown that there are early nonlinearities within the visual system prior to LM-sensitive mechanisms (He & Macleod, 1998; Legge & Foley, 1980; MacLeod, Williams, & Makous, 1992). These nonlinearities were found to be compressive and generally too weak to explain CM sensitivity (Scott-Samuel & Georgeson, 1999; Smith & Ledgeway, 1997). A compressive nonlinearity would reduce the mean luminance of high-contrast regions. Consequently, although the mean luminance of two regions varying in contrast are the same, early nonlinearities could introduce luminance variations making CM stimuli visible to LM-sensitive mechanisms. Therefore, the experimenter could erroneously conclude that a CM stimulus is processed by CM-sensitive mechanisms, although it is actually processed by LM-sensitive mechanisms following an early nonlinearity. The present experiment had two goals. First, measure the early nonlinearity for each tested condition, i.e., for each subject and each temporal frequency. Second, ensure that the processing of CM stimuli is not due to an early compressive nonlinearity and that CM stimuli were processed by CM-sensitive mechanisms in all tested conditions.

An early compressive nonlinearity may be canceled by introducing an expansive nonlinearity of the same magnitude into the stimulus (Scott-Samuel & Georgeson, 1999). The resulting nonlinearity may be defined as the sum of the early nonlinearity introduced by the visual system and the nonlinearity introduce within the stimulus. Our objective was to find the nonlinearity that needs to be introduced within the stimulus to cancel the early nonlinearity caused by the visual system. We supposed that both nonlinearities cancel one another if the same performance is observed, whether an LM and a CM signal are combined either in-phase (high contrast regions of the CM signal matching

with high luminance regions of the LM signal) or in counter-phase (high contrast regions of the CM signal matching with low luminance regions of the LM signal). Indeed, a resulting compressive nonlinearity would lower the contrast of the LM signal in the in-phase condition and would increase the contrast of the LM signal in the counter-phase condition. This would be equivalent to introducing an LM signal in counter-phase with the CM signal. Consequently, the resulting compressive nonlinearity would enhance the LM signal in the counter-phase condition and would reduce it in the in-phase condition. As a result, the performance would be greater in the counter-phase condition. Alternatively, an expansive nonlinearity would cause the opposite pattern resulting in a better performance in the in-phase condition. However, if both nonlinearities (nonlinearity of the stimulus and of the visual system) cancel one another, the same performance level should be observed, whether the LM and CM signals are combined in-phase or in counter-phase.

Method

Apparatus

The stimuli were presented on a 19-in. ViewSonic E90FB.25 CRT monitor with a mean luminance of 47 cd/m^2 and a refresh rate of 120 Hz powered by a Pentium 4 computer. The 10-bit Matrox Parhelia512 graphic card could produce 1024 grey levels that could all be presented simultaneously. The monitor was the only light source in the room. A Minolta CS100 photometer interfaced with a homemade program calibrated the output intensity of each gun. At the viewing distance of 1.14 m, the width and the height of each pixel were 1/64 deg of visual angle.

DAC precision

Although the setup used could display 1024 levels of grey, in certain conditions the contrast thresholds approached the smallest grey difference (1/1024). Since the desired luminance value for each pixel generally correspond to a continuous value, this value had to be rounded with a precision of 1/1024, i.e., to the nearest DAC value. This procedure can sometimes create sufficiently high artifacts to alter contrast threshold measurement.

Instead of simply rounding to the nearest DAC value, we used a different algorithm consisting in randomly choosing between the two nearest DAC values. The probability distribution between the two values was set so that the expected value was the desired continuous DAC value. That is, the probability of choosing the higher DAC value was equal to the remainder of the continuous desired DAC value. For example, if the desired continuous DAC value was 123.25, then the probability distribution was 0.25 for 124 and 0.75 for 123. This random selection was independently applied to each pixel of each frame.

The advantage of using such a method is that the expected luminance of each pixel of each frame is equal to the desired continuous luminance. Consequently, for a luminance grating, the expected luminance value would vary continuously, and it could therefore be possible to present a grating with a difference of luminance smaller than one DAC value (or 1/1024 of the maximal luminance). The spatiotemporal summation of a given region should result into a mean luminance value near the expected luminance. The disadvantage of this method is that it adds noise (random variations) to the presented stimulus. Thus, the noise added to the display may become a limiting factor.

This method of randomly selecting between the two nearest DAC values is mathematically equivalent to rounding to the nearest DAC value after adding dynamic noise in which each element is randomly selected from a uniform distribution varying between -0.5 and 0.5 DAC values. Since the noise sampling varied at 120 Hz and the noise contrast was small (less than 1/1024), the spectral energy of the noise was also small. To ensure that this noise had no significant impact, we measured the noise contrast required to significantly decrease the sensitivity to an LM stimulus. We found that the noise contrast required to affect sensitivity had to be at least 10 DAC values, which is much larger than the noise introduced when randomly selecting between the two nearest DAC values. We therefore concluded that the random variation introduced when randomly selecting the DAC value had no significant impact and enabled the apparatus to display a 1024 grey scale resolution equivalent to a continuous grey scale resolution.

Observers

Two psychophysically experienced observers participated in the study: one of the authors and the other naive to the purpose of the experiment. They had normal or corrected-to-normal vision.

Stimuli

For CM stimuli, binary noise is typically used as a carrier. However, one of the targets of the present study was to evaluate internal equivalent noise. Intrinsic noise within the stimulus could be a limiting factor affecting the measurement of IEN (Allard & Faubert, 2006). Consequently, we did not want the stimulus to have intrinsic noise so instead of using binary noise we used a static checkerboard as a carrier. Its contrast was set to 50%, and each check was composed of 6 × 6 pixels (5.6 × 5.6 minutes). To avoid LM cues within a check, the luminance within each check was kept spatially constant (Smith & Ledgeway, 1997). Keeping the luminance within each check spatially constant is equivalent to reducing the stimulus spatial resolution. Since the checks were small relative to the signal (21 checks per period), such lowering of the spatial resolution was judged to have no significant impact.

All the stimuli used in the present study can be defined as the sum of two terms: a luminance modulation ($M_{LM}(x, y, t)$) and the multiplication of a contrast modulation ($M_{CM}(x, y, t)$) with a static carrier ($T(x, y)$):

$$L(x,y,t) = L_0[M_{LM}(x,y,t) + M_{CM}(x,y,t)T(x,y)], \quad (1)$$

where L_0 represents the luminance average of the stimulus and the background luminance. In the present experiment, $T(x, y)$ corresponded to a static checkerboard. Its values were -0.5 if $x + y$ was odd and 0.5 otherwise resulting in a Michelson contrast of 0.5. The luminance and contrast modulations were sine wave gratings:

$$M_{LM}(x,y,t) = 1 + (C_{LM} + nC_{CM})\sin(sx + ft + p), \quad (2)$$

$$M_{CM}(x,y,t) = 1 + C_{CM}\sin(sx + ft + p), \quad (3)$$

where s, f, and p represent, respectively, the spatial frequency (0.5 cpd), the temporal frequency (varying between ±1 and ±16 Hz depending on the testing condition), and the initial phase (randomized at each trial). C_{LM} and C_{CM} represent the contrast of the LM and CM signals, which varied according to the condition. n corresponds to the nonlinearity added to the stimulus in order to compensate for early nonlinearities within the visual system. A positive nonlinearity ($n > 0$) corresponds to an expansive nonlinearity (higher luminance for higher contrast regions), while a negative nonlinearity results into a compressive nonlinearity.

A circular spatial window with a diameter of 4 deg and soft edges following a half cosine of 0.5 deg was used. Outside the carrier, the screen remained blanked to the mean luminance (L_0 = 47 cd/m^2). The presentation time was 500 ms. Between trials, when no stimulus was presented, a nonmodulated carrier was shown with a centered fixation point.

Procedure

The task consisted of discriminating the drifting direction (either left or right) of the LM or the CM signal by pressing one of two keys. To measure the compressive nonlinearity, the contrast thresholds to LM (manipulating C_{LM} and keeping C_{CM} = 0) and CM (manipulating C_{CM} and keeping C_{LM} = 0) stimuli were evaluated using a 2-down-1-up procedure (Levitt, 1971). The staircase was interrupted after sixteen inversions, and the threshold was estimated by the geometric mean of the contrast (C_{LM} or C_{CM}) at the last 8 inversions. The initial signal contrast (the dependent variable) was set significantly above threshold. The step size before the second inversion was 0.2 log units. Afterwards and until the forth inversions, it was set to 0.1 log units. Subsequent to the forth inversion the step size was 0.05 log units.

It was important to properly evaluate the LM and CM contrast thresholds since the settings of the next procedural step depended on them. Large measurement errors could compromise the next procedural step consisting in measuring the compressive nonlinearity of the visual system. To enhance threshold precision, LM and CM thresholds were evaluated three times (three staircases) for each temporal frequency. Each threshold was estimated as the geometric mean of the three staircases.

For each temporal frequency, once the contrast thresholds to LM (C_{LM}) and CM (C_{CM}) stimuli were measured (which we will denote T_{LM} and T_{CM}, respectively), the expansive nonlinearity that needed to be introduced within the stimulus (n) to compensate for the compressive nonlinearity of the visual system was evaluated. To do so, the performance level (proportion of correct answers) was evaluated when superimposing LM and CM signals at threshold either in-phase ($C_{LM} = T_{LM}$ and $C_{CM} = T_{CM}$) or in counter-phase ($C_{LM} = T_{LM}$ and $C_{CM} = -T_{CM}$). For each of these two phase conditions, five nonlinearities (n) were added. As mentioned above, the nonlinearity was an additional LM signal in-phase with the CM signal with contrast nC_{CM}. For comparative reasons, we also evaluated the performance level to LM ($C_{LM} = T_{LM}$ and $C_{CM} = 0$) and CM ($C_{LM} = 0$ and $C_{CM} = T_{CM}$) signals separately. Overall, performance was evaluated for twelve stimuli: the combination of LM and CM signals in-phase using 5 different nonlinearities, the combination of LM and CM signals in counter-phase using the same 5 different nonlinearities, an LM signal alone and a CM signal alone using one nonlinearity. The five nonlinearities for the combined signals and the nonlinearity for the CM signal alone were arbitrarily set based on a pilot study. There values can be seen in the Figure 1 of the next section. For each performance level evaluated, 50 trials were performed resulting in 600 trials presented in a pseudo-random order.

Fitting the data

Two normalized cumulative Gaussian functions were fitted to the data for each temporal frequency of each subject. For the in-phase condition, the function increased with the nonlinearity, and for the counter-phase condition, the function decreased with the nonlinearity. Both functions were constrained to have the same slope, the same lower bound and an upper bound set to 100% correct response. The lower bound was not fixed because it consisted in the performance for CM stimuli alone.

Results and discussion

Early nonlinearity measured

The estimated stimulus nonlinearities needed to compensate for early nonlinearities of the visual system are

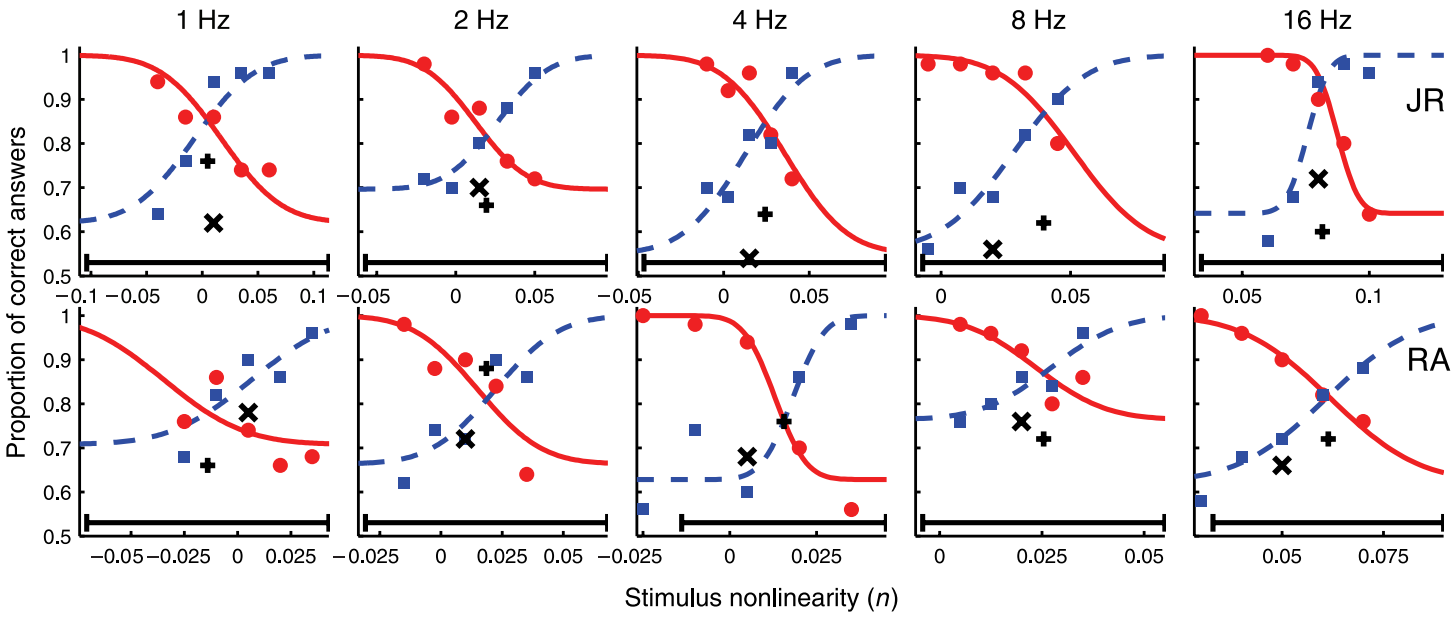

Figure 1. Nonlinearity results. The blue squares and red dots correspond to the percentage of correct answers when LM and CM stimuli were combined in-phase and in counter-phase, respectively. The black horizontal lines represent the range of nonlinearity added to the stimulus within which CM stimuli must be processed by CM-sensitive mechanisms. The + and × signs correspond to the performance level when only LM and CM signals were presented alone, respectively. For LM signals alone, the nonlinearity added is undefined so we arbitrarily set the position of the + signs to the measured nonlinearity compensating for the early compressive nonlinearity. For CM signals, the nonlinearity added was arbitrarily set and is shown by the horizontal position of the × signs.

presented in Figure 1. As described above, the same performance observed whether LM and CM signals are combined in-phase or in counter-phase (the point at which the two lines cross in Figure 1) suggests that the early nonlinearity of the visual system was compensated by the nonlinearity added to the stimulus. As previously observed (Scott-Samuel & Georgeson, 1999; Smith & Ledgeway, 1997), at low temporal frequencies, early nonlinearities of the visual system were small ($n \approx 0$). However, at greater temporal frequencies, early nonlinearities were greater and compressive. Indeed, expansive nonlinearities ($n > 0$) had to be added to compensate for the early nonlinearities of the visual system.

Modeling the nonlinearity of the visual system

Scott-Samuel and Georgeson (1999) have used the Naka–Rushton equation with the exponent variable set to 1 to model the compressive nonlinearity of the visual system. Using this function, the intensity of the photoreceptor response relative to the maximal response can be modeled by the following function:

$$E(x,y,t) = \frac{L(x,y,t)/L_0}{L(x,y,t)/L_0 + S}. \quad (4)$$

The compressive nonlinearity of the retinal receptors depends on the parameter S. To fit the parameter S, we have used a similar approach as Scott-Samuel and Georgeson (1999). For each conditions (i.e., each temporal frequency and each subject), we created two stimuli composed of an LM and a CM signal either combined in-phase ($C_{LM} = T_{LM}$) or in counter-phase ($C_{LM} = -T_{LM}$) using the stimulus nonlinearity (n) at which the same performance was observed whether the signals were combined in-phase or in counter-phase. The contrast of the CM signal was also equal to the threshold ($C_{CM} = T_{CM}$). The compressive nonlinearity of the visual system was modeled by applying Equation 4 to each stimulus. The S variable was manipulated until the Fourier transform of the two stimuli gave the same spectral energy at the signal frequency. If the observer has the same performance whether the LM and CM signal are combined in-phase or in counter-phase, we concluded that the compressive nonlinearity was compensated by the expansive nonlinearity induced in the stimulus.

We did not model the nonlinearity at 1 and 2 Hz since the nonlinearities measured were too low ($n \approx 0$) to have a significant impact on the results of the next experiments. At 4 Hz, the fitted S values were 19 and 20 for observer JR and RA, respectively. At 8 Hz, they were 7.2 and 11.5, respectively. And at 16 Hz, they were 5.2 and 7.1, respectively. Lower values for the S parameter represent higher compressive nonlinearities. The increasing nonlinearity observed when increasing the temporal frequency is consistent with Scott-Samuel and Georgeson's (1999) results. However, the nonlinearities observed at 16 Hz

were lower than what has been previously observed. Near this temporal frequency, nonlinearities were found to vary between 0.5 and 3.5 (Scott-Samuel & Georgeson, 1999). However, a pilot study showed that leaving the carrier visible between trials reduced the nonlinearity, suggesting that the stimulus onset enhances compressive nonlinearities of the visual system. This is consistent with the fact that the nonlinearity decreases with increasing presentation time as suggested by Scott-Samuel and Georgeson.

Once the S parameter was estimated for each testing condition, we compared the difference between using the Naka–Rushton equation (Equation 4) and simply adding a luminance modulation proportional to the contrast modulation using the parameter n (Equation 2). To compare these models, we created stimuli composed of either a unique CM signal at different contrasts ($C_{LM} = 0$ and $C_{CM} = 0$ to 0.9) or a unique LM signal equal to the discrimination threshold ($C_{LM} = T_{LM}$ and $C_{CM} = 0$). The nonlinearity (n) applied to the stimuli was the one estimated by fitting the data as shown in Figure 1. The modeled nonlinearity was then applied to each one of them using Equation 4 with the estimated S parameter. Afterwards, we evaluated the energy at the envelope spatiotemporal frequency by applying the Fourier transform to each stimulus. In all the conditions, we found that the energy induced by the CM signal was always orders of magnitude lower than the energy induced by the LM signal. In other words, the difference between modeling early nonlinearities using the Naka–Rushton equation and simply adding a luminance modulation proportional to the contrast modulation was too weak to generate a detectable LM signal, and this, at any contrast level. We therefore concluded that even when CM stimuli were presented well above threshold, they were processed by CM-sensitive mechanisms and not LM-sensitive mechanisms due to a global distortion artifact.

CM-sensitive mechanisms

As mentioned above, the resulting nonlinearity may be defined as the sum of the nonlinearity added to the stimulus, and the early nonlinearity added by the visual system. When one is the inverse of the other (one expansive and the other compressive with the same magnitude), the resulting nonlinearity is 0. However, when they differ, an LM signal is added to the effective stimulus (the resulting stimulus after applying the early nonlinearity of the visual system). If the difference is strong enough (contrast of an LM signal induced by the resulting nonlinearity greater than the contrast threshold to LM stimuli), then LM-sensitive mechanisms could process such artifact. The black horizontal line in Figure 1 represents the range within which CM stimuli must be processed by CM-sensitive mechanisms. This range was calculated as the stimulus nonlinearity canceling the early nonlinearity of the visual system (where the two lines cross) ± the LM/CM contrast threshold ratio (T_{LM}/T_{CM}). Consequently, within this range, the performance level observed when presenting a CM signal alone is not due to an early nonlinearity permitting the LM-sensitive mechanisms to process CM signals.

The × signs shown in Figure 1 correspond to the proportion of correct answers to CM stimuli presented alone ($C_{LM} = 0$) with a nonlinearity added to the stimulus. As described above, the nonlinearity added was arbitrarily set based on a pilot study. This value is shown by the × positions on the horizontal axis. As it can be observed, all × signs are within the range in which CM stimuli must be processed by CM-sensitive mechanisms (horizontal black line). Furthermore, the proportion of correct answers to CM stimuli presented alone (that is, with a nonlinearity but without an LM signal) are all above chance level (50%). We therefore conclude that at all temporal frequencies tested there are mechanisms sensitive to CM stimuli even if we compensate for early nonlinearities. This does not imply that the mechanisms processing LM and CM stimuli are distinct. A mechanism sensitive to CM stimuli could also be sensitive to LM stimuli. These results rather imply that, in these conditions, CM stimuli were not processed by mechanisms only sensitive to LM stimuli after being distorted by an early nonlinearity introducing an LM signal within a CM stimulus.

Phase independent test

The + signs shown in Figure 1 correspond to the proportion of correct answers when presenting an LM stimulus alone. For such stimuli, the nonlinearity added to the stimulus (n) has no impact since there was no CM signal ($C_{CM} = 0$). Consequently, there is no defined position on the horizontal axis for LM signals presented alone. We arbitrarily chose to set the position on this axis for LM signals presented alone to the measured compensating nonlinearity (where the two lines cross).

When compensating for the early nonlinearity of the visual system, the proportion of correct answers to the combination of LM and CM signals either in-phase or in counter-phase (performance level where the two fitted lines cross) was generally greater than, or close to, the proportion of correct answers to LM or CM signals alone (+ and × signs). Consequently, in all the temporal frequencies tested, we conclude that there are CM-sensitive mechanisms able to discriminate the motion direction. Indeed, if CM stimuli could only be detected due to an early nonlinearity within the visual system, then LM and CM signals should cancel one another either when combined in-phase or in counter-phase (Lu & Sperling, 1995, 2001). However, the opposite pattern was observed: combining both either in-phase or in counter-phase generally results in a better performance.

Similar results showing that there are CM-sensitive mechanisms even up to 15 Hz have been previously found

(Scott-Samuel & Georgeson, 1999). However, it was important to replicate similar experiments to measure the early nonlinearity of the visual system at each temporal frequency of each subject, and to show that with the parameters used and at all temporal frequencies tested, CM stimuli were processed by CM-sensitive mechanisms, not by LM-sensitive mechanisms following an early nonlinearity. Again, this does not mean that LM and CM stimuli are processed by separate mechanisms. It rather implies that even if we compensate for early nonlinearities, there are mechanisms sensitive to CM stimuli.

Experiment 2: Inter-attribute interaction

We previously found no or little inter-attribute interaction between LM and CM static stimuli processing (Allard & Faubert, 2007). LM noise affected LM signal detection but had little or no impact on CM signal detection and, vice versa, CM noise affected CM signal but had little or no impact on LM signal detection. This double dissociation strongly suggests that LM and CM signals are detected, at least at some point, by separate mechanisms.

In another study (Allard & Faubert, 2006), we also found similar detection thresholds for LM and CM stimuli embedded in high LM and CM noise, respectively; that is, similar CEs but different IENs were obtained for detecting static LM and CM stimuli. In other words, observers were just as efficient at detecting LM signals embedded in LM noise as detecting CM signals embedded in CM noise.

The main purpose of the second experiment was to apply a similar noise masking paradigm to LM and CM motion processing. We therefore evaluated the contrast thresholds of LM and CM stimuli embedded in LM and CM noise.

Method

Many aspects of the methodology used in the second experiment were the same as the ones used in the previous experiment. In the current section, only their differences are presented.

Stimuli

The modulation functions defining the stimuli in the previous experiment (Equations 2 and 3) were altered in order to add LM and CM noise to the stimulus. Consequently, an extra term corresponding to the noise function ($N(x, y, t)$) was added. Similarly to the signal (the two sine wave gratings), the noise could either be LM or CM:

$$M_{\mathrm{LM}}(x,y,t) = 1 + (C_{\mathrm{LM}} + nC_{\mathrm{CM}})\sin(sx + ft + p) + (N_{\mathrm{LM}} + nN_{\mathrm{CM}})N(x,y,t), \quad (5)$$

$$M_{\mathrm{CM}}(x,y,t) = 1 + C_{\mathrm{CM}}\sin(sx + ft + p) + N_{\mathrm{CM}}N(x,y,t), \quad (6)$$

where N_{LM} and N_{CM} correspond to the contrast of the LM and CM noise, respectively. nN_{CM} corresponds to an LM noise added to compensate for the early nonlinearity within the visual system. We supposed that the proportion of CM information being converted into LM information by an early nonlinearity of the visual system is the same for the signal and noise. We therefore simply applied a linear model to compensate the nonlinearity of the visual system in which we supposed that the LM function was proportional (by a factor of n) to the CM function. $N(x, y, t)$ represents the noise function defined as filtered noise following a Gaussian distribution centered on 0 and with a root mean square of 1 after being filtered. The noise was filtered in the Fourier domain by an ideal mask keeping only the temporal and spatial frequencies within one octave below and above the frequency of the signal. Movie 2 illustrates examples of LM and CM noise.

Procedure

For each temporal frequency, thresholds for LM and CM signals (C_{LM} and C_{CM}, respectively) were evaluated

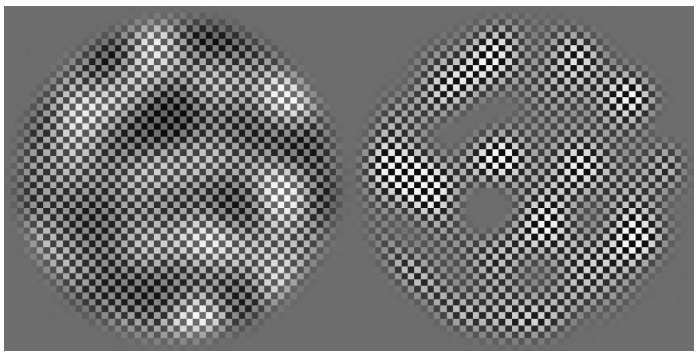

Movie 2. LM (left) and CM (right) noise. The noise was filtered 1 octave above and below the spatiotemporal frequency of the signal. The spatial frequency of the signal was always 0.5 cpd, i.e., the frequencies within 0.25 and 1 cpd were kept. The temporal frequency varied from one condition to another. In the present example, only the temporal frequencies within 1 and 4 Hz were kept.

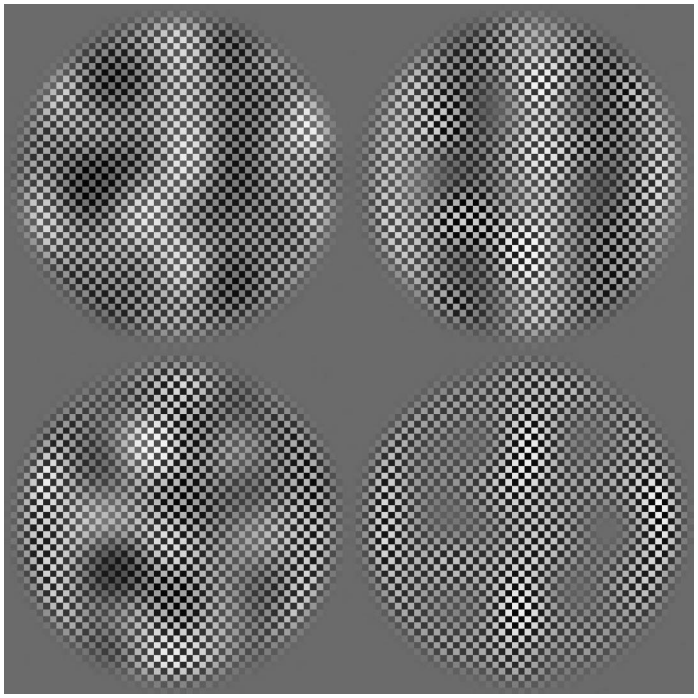

Movie 3. LM and CM signal embedded in LM and CM noise. In the top row, the signals are LM. In the bottom row, the signals are CM. In the left column, the noise is LM. In the right column, the noise is CM.

in five different levels of either LM noise (N_{LM} = 0.0088, 0.018, 0.035, 0.071, and 0.14) or CM noise (N_{CM} = 0.071, 0.10, 0.14, 0.20, and 0.28). Each threshold was measured using one staircase controlling either C_{LM} or C_{CM} (the other parameter was fixed to 0) as described in the previous experiment. The order of the testing was blocked relative to the temporal frequencies, but the order of the 20 thresholds for one block (4 signal-noise conditions (Movie 3) and 5 noise levels) was randomized. For each temporal frequency, the nonlinearity (n) induced within the stimulus was the one measured in the previous experiment.

Results and discussion

Calculation efficiency

Figure 2 shows the results for LM and CM thresholds embedded in LM and CM noise, respectively. These results were fitted using the TvC function (for details, see Allard & Faubert, 2006) known to give a good fit for contrast thresholds as a function of noise contrast when the signal and noise are of the same type (Legge et al., 1987; Pelli, 1981, 1990; Pelli & Farell, 1999). In certain conditions, even at the highest CM noise level, CM thresholds were hardly affected by the noise (especially for observer JR at 16 Hz). These data result in a good fit for flat portion of the TvC function but give a poor fit for the rising part of the function. To improve the fit, we introduced an extra constraint: The calculation efficiency to CM stimuli could not be greater than the calculation efficiency to LM stimuli. In other words, the rising parts of the TvC functions of the blue dashed lines fitting CM thresholds in Figure 2 were constrained to be equal or above the rising parts of the red solid lines fitting LM thresholds. This constraint had no or little impact in almost all the conditions. However, without it at 16 Hz for observer JR, the fit resulted in a straight line corresponding

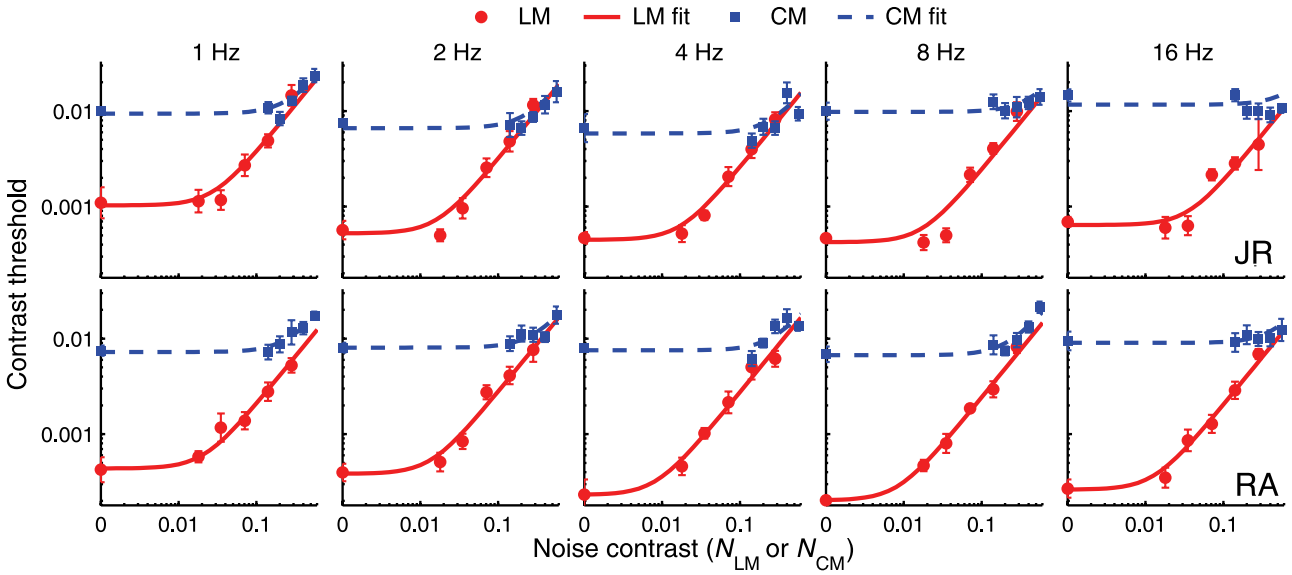

Figure 2. Motion discrimination in intra-attribute noise. Red dots and solid lines correspond to LM contrast thresholds in LM noise (raw data and fitted TvC function, respectively). Blue squares and dashed lines correspond to CM contrast thresholds in CM noise. Error bars correspond to the standard deviation from the mean.

to extremely high calculation efficiency and internal equivalent noise. For this condition, the data were only driven by the flat portion of the TvC function, which only gives a lower bound to the internal equivalent noise and calculation efficiency. However, we know of no models suggesting that we could be more sensitive to a given signal embedded in noise when both are CM rather than LM. We therefore think that this extra constraint is justified and enables the fit to set a lower bound to the calculation efficiency to CM stimuli when the highest noise contrast did not significantly affect the threshold.

As expected, LM and CM thresholds largely differed in the absence of noise. However, when the noise was sufficiently high, there was no or little threshold difference between LM and CM signals. In other words, observers were just as efficient at discriminating the direction of an LM signal in LM noise as for a CM signal in CM noise. Consequently, observers had similar calculation efficiencies to both attributes, and this, for a wide temporal frequency range. These results therefore suggest that, for LM and CM stimuli, common mechanisms could be extracting the signal from noise.

Internal equivalent noise

Since the difference of sensitivity to LM and CM stimuli processing was not due to a difference of CE, it was obviously due to a difference of IEN corresponding to the breaking point on the TvC function. As mentioned in the introduction, similar results were obtained for static stimuli (Allard & Faubert, 2006), which led us to suggest that the difference of IEN could be due to a suboptimal rectification process for CM stimuli. However, based on the difference of IEN, one cannot conclude that both attributes are processed by separate mechanisms. If both stimuli are processed by common mechanisms, then the difference of sensitivity would likely be due to different contrast gains. Different contrast gains prior to the main noise source would increase the relative impact of the main noise source and thereby affect the observer's threshold. However, if the main noise source is external (when the external noise is greater than the IEN), the contrast gain would affect both the signal and noise contrasts without affecting the signal-to-noise ratio. Consequently, in high noise conditions, the threshold would be independent of the contrast gain. As a result, one cannot conclude that two stimuli are processed by separate mechanisms simply based on different IENs since the common mechanism hypothesis would also predict this pattern of results.

CM processing in LM noise

At 16 Hz, LM noise affected both LM and CM thresholds by similar proportions (Figure 3). In other words, LM noise had the same relative impact on LM and CM thresholds. Although the noise was band-pass at one octave below and above the signal spatiotemporal frequencies, the noise did not selectively impair LM processing without having the same impact on CM processing. In other words, the smallest LM noise

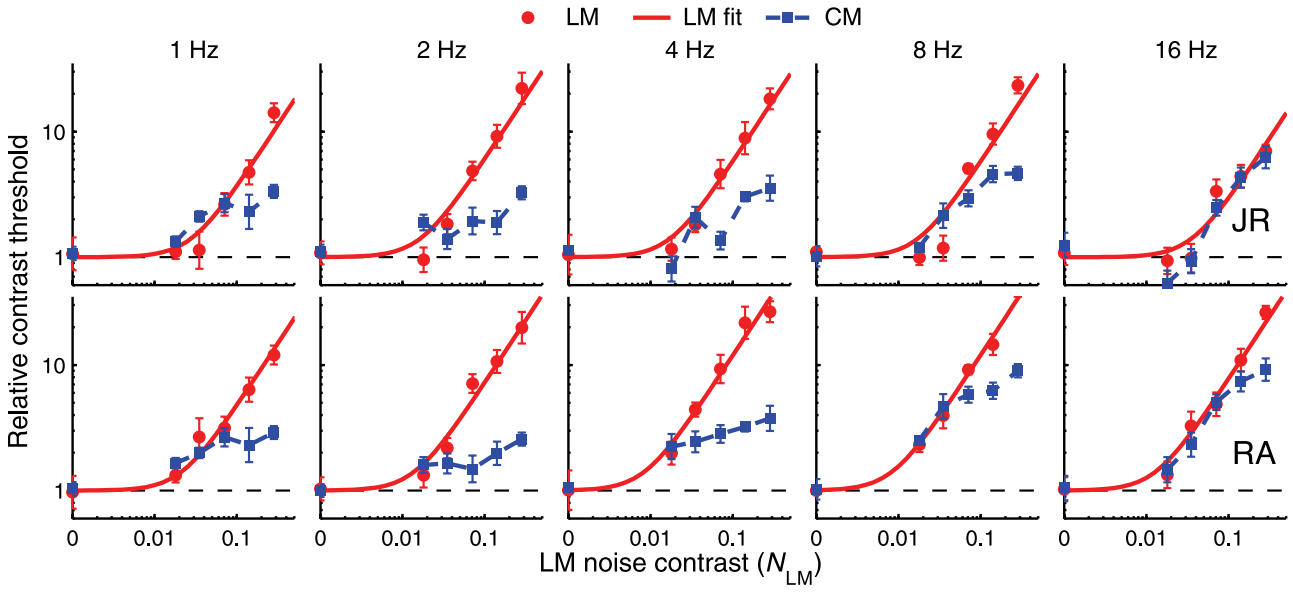

Figure 3. LM and CM relative contrast thresholds as a function of LM noise contrast. Contrast thresholds are represented relative to their contrast thresholds in absence of noise fitted by the TvC function (where the fitted curves cross the *y*-axis in Figure 2). For LM stimuli, the thresholds and best fitted TvC functions are represented (red dots and solid lines, respectively). For CM stimuli, since the external noise was not of the same type, we could not fit the TvC function and only the evaluated thresholds are represented (blue squares). Error bars corresponds to the standard deviation from the mean.

contrast significantly affecting CM thresholds matches the one affecting LM thresholds and is highly different from the smallest CM noise contrast significantly affecting CM thresholds shown in Figure 2. This suggests that, at 16 Hz, LM and CM stimuli are processed by common mechanisms.

At 8 Hz, a similar pattern of results was observed for external noise contrasts affecting LM or CM thresholds by a factor less than 3 or 4 (Figure 3). This suggests that, at 8 Hz, LM and CM signals are processed by common mechanisms since both attributes were affected by similar proportions. Above this critical value, CM thresholds were less affected by LM noise than LM thresholds. This suggests the existence of separate mechanisms processing LM and CM signals. Taken together, these results suggest that two mechanisms could be processing CM stimuli. The more sensitive one (the one processing CM stimuli at 8 Hz in noiseless conditions) would be common to LM processing. However, the less sensitive one (here by a factor of about 3 or 4) would not be common to LM processing explaining why high LM noise contrasts affected more LM than CM processing at 8 Hz.

At lower temporal frequencies (1, 2, and 4 Hz), CM processing was generally less affected by LM noise than LM processing (Figure 3). Indeed, the two curves had the tendency to split at the point where thresholds increased by a factor of about 3, 1.5, and 2 for the temporal frequencies 1, 2, and 4 Hz, respectively. This suggests that, at least in high LM noise conditions, LM and CM signals are processed by separate mechanisms.

LM processing in CM noise

Unfortunately, even in high CM noise, the impact of the noise on CM processing was relatively limited (Figure 4). Consequently, it was not possible to have sufficient noise contrast to severely impair CM processing. However, since at the highest noise contrast CM processing was generally significantly affected, the impact on LM processing could also be evaluated. At temporal frequencies at or above 4 Hz, LM processing seemed to be affected in similar proportions as CM processing (except at 16 Hz for subject JR, whose LM and CM thresholds remained unaffected by the highest CM noise contrast). These results also support the hypothesis that both LM and CM stimuli are processed by common mechanisms at high temporal frequencies.

At lower temporal frequencies (1 and 2 Hz), LM processing was generally less affected than CM processing (Figure 4). Indeed, at these temporal frequencies, CM noise impaired CM processing more than LM processing suggesting that both attributes are processed by separate mechanisms.

Experiment 3: Carrier and nonlinearity control

Even though component motion could not explain the results obtained in the previous experiment, the choice of a periodic carrier remains an issue. For instance, a

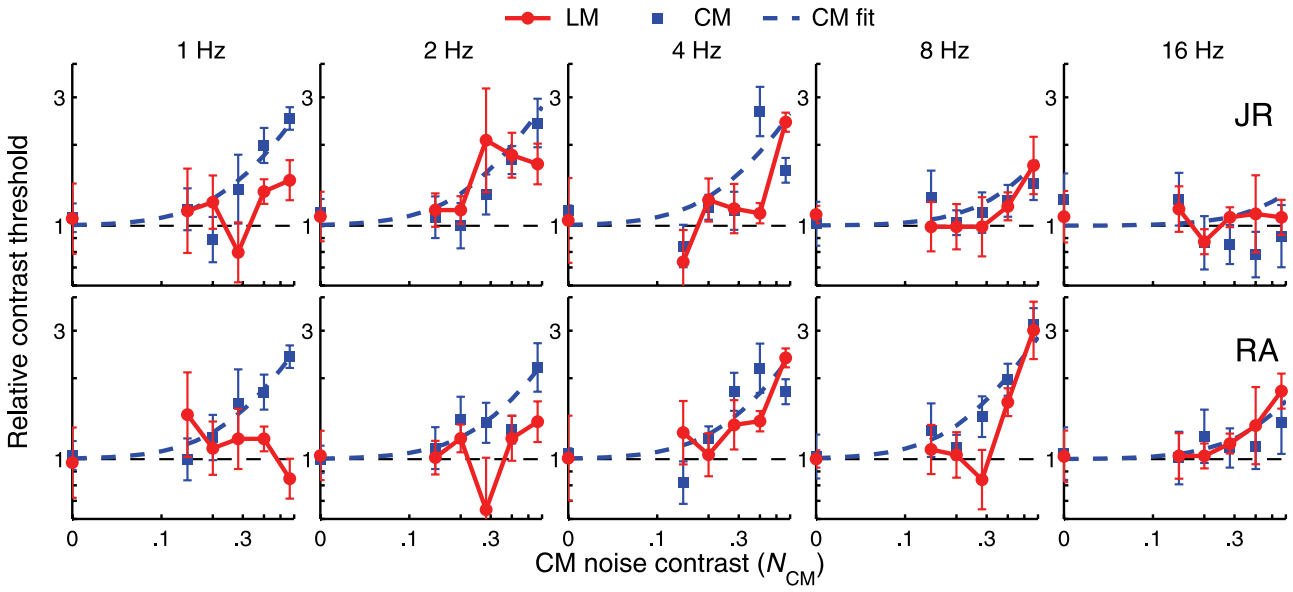

Figure 4. LM and CM relative contrast thresholds as a function of CM noise contrast. Contrast thresholds are represented relative to their contrast thresholds in absence of noise fitted by the TvC function (where the fitted curves cross the *y*-axis in Figure 2). For CM stimuli, the thresholds and best fitted TvC functions are represented (blue squares and dashed lines, respectively). For LM stimuli, since the external noise was not of the same type, we could not fit the TvC function, and only the evaluated thresholds are represented (red circles). Error bars corresponds to the standard deviation from the mean.

checkerboard carrier has constant luminance along the diagonals. Some could therefore argue that CM stimuli have luminance modulations along these diagonals that could be detected by LM-sensitive mechanisms. However, the use of relatively small check size (21 checks per signal cycles) should minimize such artifacts. Nonetheless, many experimenters prefer using noise as a carrier rather than a regular structure.

Smith and Ledgeway (1997) have shown that using static binary noise carriers with large element size can give rise to local first-order artifacts as described in Experiment 1. They suggested the used of either dynamic broadband noise or static high-pass noise. An important disadvantage of using dynamic noise for our purpose is that the noise introduced by the carrier would affect contrast thresholds to both LM and CM stimuli, which thereby reduces the impact of adding LM or CM noise. We therefore conducted a control experiment using static high-pass noise as a carrier.

Another artifact that could have influenced our results at high temporal frequencies is if the nonlinearity of the visual system was not well compensated for by the proportional nonlinearity applied to the stimulus resulting into a global distortion product. Indeed, we measured the nonlinearity at threshold and then supposed that the nonlinearity induced by the visual system was proportional to the CM signal contrast. Scott-Samuel and Georgeson (1999) suggested using the Naka–Rushton equation to compensate for the visual system nonlinearities. Even though we have demonstrated using simulations in Experiment 1 that the difference between the two models are too small to affect our results, the presence of LM or CM noise could affect the compressive nonlinearity. As a result, it could be argued that our results suggesting common mechanisms at high temporal frequency could be due to a global distortion product that would be different in noise conditions. The present experiment focused on a low (2 Hz) and a high (8 Hz) temporal frequency. We evaluated LM and CM discrimination thresholds in noiseless, LM and CM noise conditions. In order to assert that the results at 8 Hz were not due to some global distortion product, we directly measured the compressive nonlinearity in all three conditions, i.e., no noise, LM noise, and CM noise.

Method

Many aspects of the methodology used in the present experiment were the same to the ones used in the previous experiments. In the current section, only their differences are presented.

Stimuli

The stimuli used were similar to the ones in the previous experiment with the exception of the carrier

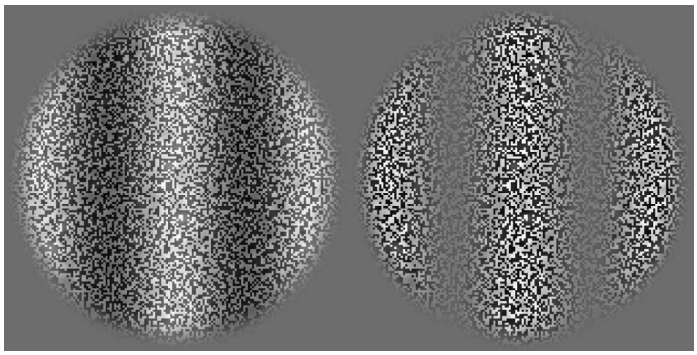

Movie 4. LM (left) and CM (right) drifting grating at 2 Hz. The carrier corresponds to binary noise that was filtered to keep only the frequencies above 4 cpd.

($T(x, y)$). The carrier was generated by creating a binary noise texture ($T(x, y) = -0.5$ or 0.5) with element size equal to 2×2 pixels, which was then high-pass filtered with a cutoff frequency at 4 cpd (Movie 4). Such filtering had little impact on the RMS contrast of the carrier reducing it by 3%.

Procedure

For each temporal frequency (2 and 8 Hz), LM and CM direction discrimination thresholds were evaluated in noiseless conditions, LM noise ($N_{LM} = 0.020$) and in CM noise ($N_{CM} = 0.28$). Note that the LM noise was not set to its maximal contrast. We chose the noise contrast based on the results obtained at 8 Hz of the previous experiment such that both LM and CM detection thresholds were affected by similar proportions. As discussed in the previous experiment, when the LM noise contrast was too high, CM thresholds were less affected than LM thresholds suggesting that another mechanism was able to process CM stimuli. The same noise contrast was used at both temporal frequencies. Each threshold was evaluated three times using the 2-down-1-up staircase as described in the first experiment.

In Experiment 1, we found that the compressive nonlinearity of the visual system was too weak at 2 Hz to introduce global first-order artifacts within CM stimuli that would be detectable by LM-sensitive mechanisms. In the current experiment, we therefore did not measure the compressive nonlinearity and assumed that it was null ($n = 0$). The double dissociation observed (see Results and discussion section) ensures that the nonlinearities of the visual system did not affect the results.

Since we expected complete inter-attribute interactions at 8 Hz, it was important to ensure that the results were not due to compressive nonlinearities introducing LM signals within CM stimuli. Instead of applying the inverse of a given retinal model (e.g., Naka–Rushton

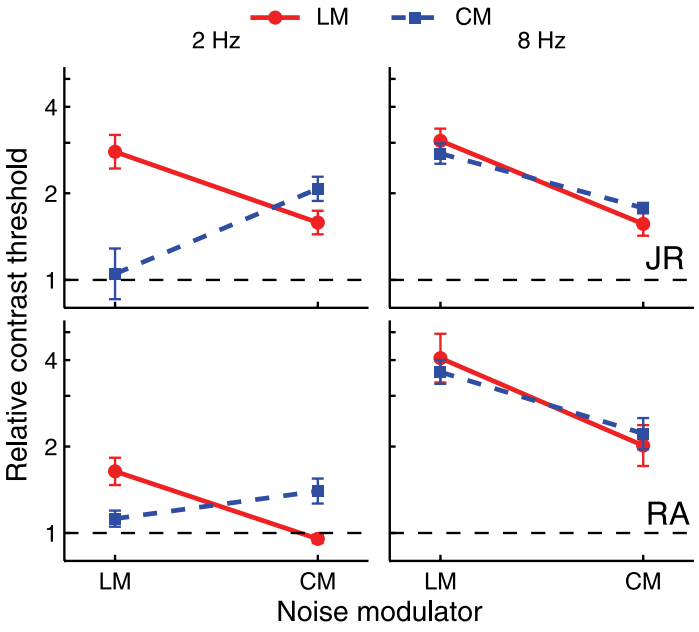

Figure 5. Impact of LM and CM noise on LM and CM thresholds at 2 Hz (left) and 8 Hz (right) for observers JR (top) and RA (bottom). The *y*-axis shows the contrast thresholds relative to contrast threshold in absence of noise. The *x*-axis represents the type of noise added to the stimulus (LM or CM). Error bars show standard error of the three thresholds measured for each condition.

equation) to compensate for early nonlinearities, we used the proportional model as in the first two experiments and directly measured the nonlinearity in all three noise conditions (no noise, LM noise, and CM noise). We therefore measured the compressive nonlinearity of the visual system for each observer and applied the inverse nonlinearity (parameter n) to the stimulus as done in the previous experiments. Afterwards, the nonlinearity was reevaluated for each noise conditions to show that in all conditions the global distortion product was too low to explain our results.

Results and discussion

Separate mechanisms at low temporal frequencies

At 2 Hz, LM noise had a significantly greater impact on LM processing than on CM processing for both observers and CM noise had a significantly greater impact on CM processing than on LM processing (Figure 5, left). This double dissociation confirms the results obtained in the previous experiment, strongly suggesting that both attributes are processed by separate mechanisms. Indeed, the fact that it was possible to selectively impair either processing implies that both must be processed, at least at some point, by separate mechanisms.

Common mechanisms at high temporal frequencies

At 8 Hz, a completely different pattern of results was observed (Figure 5 right), LM and CM noises each affected LM and CM processing by similar proportions. These complete inter-attribute interactions suggest that both attributes are processed by common mechanisms at high temporal frequencies.

Figure 6 shows the nonlinearity measured for each of the noise conditions. The stimulus nonlinearities in noiseless conditions found to compensate for early nonlinearities of the visual system (n = 0.022 and 0.014 for observers JR

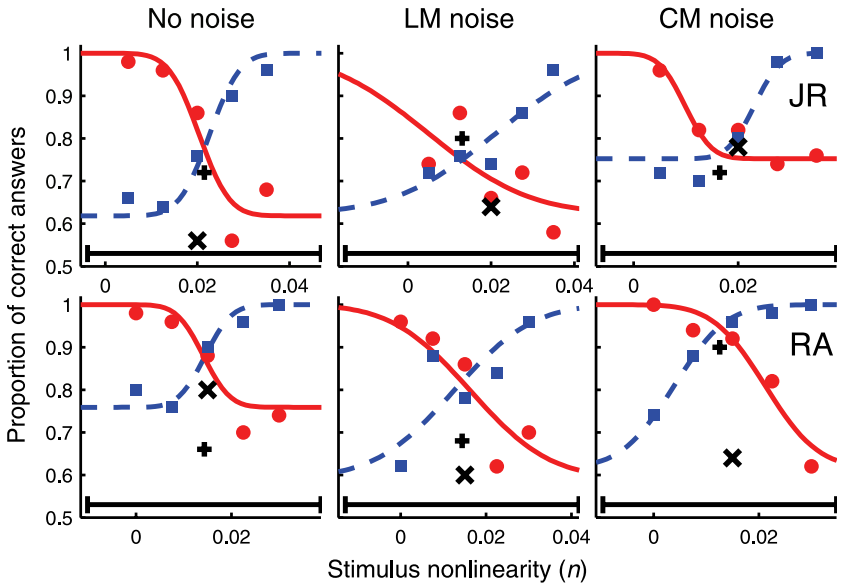

Figure 6. Nonlinearity results at 8 Hz in three different noise conditions: no noise (left), LM noise (center), and CM noise (right). The legend is the same as the one described in the caption of Figure 1.

for high temporal frequencies, a mechanism sensitive to an LM signal at a given spatial frequency would also be sensitive to CM stimuli based on the envelope spatial frequency. We therefore conclude that both attributes are processed by fundamentally distinct mechanisms when a double dissociation is observed. Indeed, a model suggesting that both attributes are processed by common mechanisms at all processing levels, such as the gradient-based model, could not explain both the double dissociation at low temporal frequencies and the complete interaction at high temporal frequencies.

As seen above, the dissociations between LM and CM processing were more important at low temporal frequencies. This suggests that the dedicated mechanisms processing LM and CM stimuli are more sensitive at low temporal frequencies. Combining these results with the fact that cross-attribute noise has little or no impact on spatial processing (Allard & Faubert, 2006) suggests that the separate mechanisms processing LM and CM stimuli first need to extract spatial information before processing motion. The filter–rectify–filter model suggesting that both attributes are initially processed by separate mechanisms also proposes that the spatial structure of CM stimuli is first extracted (rectification process) before evaluating the motion direction. This initial spatial processing stage could explain why such mechanisms would be more sensitive at low temporal frequencies. Indeed, the sensitivity to most second-order stimuli defined by attributes other than contrast, such as by depth (Lu & Sperling, 1995) or polarity reversals (Bellefeuille & Faubert, 1998; Hutchinson & Ledgeway, 2006), is generally found to be temporally low-pass. After the rectification process (or any process extracting the spatial structure of the envelope), moving CM stimuli could either be processed by an energy-based mechanism dedicated to second-order processing or by a feature tracking mechanism comparing the spatial position of the envelope in time. Our results do not enable us to dissociate these models. Based on other studies, we addressed this question in the following section.

Motion processing of CM stimuli

We are not the firsts to suggest that CM stimuli can be processed by fundamentally different mechanisms depending on the testing parameters (here the temporal frequency). Seiffert and Cavanagh (1999) evaluated whether CM stimuli are processed by an energy-based or a position-based mechanism by measuring motion amplitude thresholds of oscillating gratings. They concluded that CM stimuli could be processed by either mechanism. An energy-based mechanism would be more sensitive to CM stimuli at high temporal frequencies and high carrier contrasts, and a position-based mechanism would be more sensitive at low temporal frequencies and low carrier contrasts. A position-based mechanism would first require spatial processing in order to extract the spatial properties of the signal and then compare its positions at different time intervals. Their results are in agreement with ours given that LM stimuli are always processed by energy-based mechanisms (Zaidi & DeBonet, 2000). At low temporal frequencies, CM stimuli would be processed by a position-based mechanism once the spatial structure has been extracted. At high temporal frequencies, LM and CM stimuli would be processed by common energy-based mechanisms. Note that equivalence between gradient- and energy-based models have been shown (Benton, 2004). Indeed, Benton (2004) demonstrated that energy-based models combined with a subsequent contrast normalization process could discriminate the motion direction of CM stimuli.

Ukkonen and Derrington (2000) suggested similar conclusions using the pedestal test (Lu & Sperling, 1995) to evaluate whether the carrier contrast is processed by feature tracking mechanisms or by spatiotemporal filters. Using a low contrast carrier, they found that CM stimuli processing did not pass the pedestal test and was only possible at low temporal frequencies (<4 Hz). They concluded that when using a low contrast carrier, CM stimuli are processed by a feature tracking mechanism. On the other hand, when using a high contrast carrier, CM stimuli processing was unaffected by the pedestal and could be processed at higher temporal frequencies (up to the highest frequency tested of 12 Hz). They conclude that CM stimuli are processed by spatiotemporal filters when using a high contrast carrier. Again, these results are in agreement with ours. There could be two types of mechanisms processing CM stimuli, one low-pass initially extracting the spatial structure of the envelope and another which, we suggest, could be common to LM processing.

These studies show that CM stimuli could be processed by feature tracking (or position-based) mechanisms and by energy-based mechanisms depending on the stimulus conditions. At high temporal frequencies and high carrier contrasts, the energy-based mechanism would be more sensitive to CM stimuli than the feature tracking mechanism. At low temporal frequencies and low carrier contrasts, the feature tracking mechanism would be more sensitive. Since our results suggest that LM and CM stimuli are processed by common mechanisms at high temporal frequencies and that LM-sensitive mechanisms are known to be energy-based, our results also suggest that CM stimuli are processed by energy-based mechanisms. Since LM stimuli are always processed by energy-based mechanisms, the results obtained by Ukkonnen and Derington and Seiffert and Cavanagh showing that CM stimuli are processed by a feature tracking (or position-based) mechanism at low temporal frequencies also suggests that LM and CM stimuli are processed by separate mechanism and are consistent with our results. Consequently, this suggests that when a double dissociation was observed, CM stimuli were processed by a feature tracking mechanism. To explain our results, there

Johnston, A., Benton, C. P., & McOwan, P. W. (1999). Induced motion at texture-defined motion boundaries. *Proceedings of the Royal Society B: Biological Sciences, 266,* 2441–2450. [PubMed] [Article]

Johnston, A., & Clifford, C. W. (1995). Perceived motion of contrast-modulated gratings: Predictions of the multi-channel gradient model and the role of full-wave rectification. *Vision Research, 35,* 1771–1783. [PubMed]

Johnston, A., McOwan, P. W., & Buxton, H. (1992). A computational model of the analysis of some first-order and second-order motion patterns by simple and complex cells. *Proceedings of the Royal Society B: Biological Sciences, 250,* 297–306. [PubMed]

Legge, G. E., & Foley, J. M. (1980). Contrast masking in human vision. *Journal of the Optical Society of America, 70,* 1458–1471. [PubMed]

Legge, G. E., Kersten, D., & Burgess, A. E. (1987). Contrast discrimination in noise. *Journal of the Optical Society of America A, Optics and Image Science, 4,* 391–404. [PubMed]

Levitt, H. (1971). Transformed up-down methods in psychoacoustics. *Journal of the Acoustical Society of America, 49,* 467+. [PubMed]

Lu, Z. L., & Sperling, G. (1995). The functional architecture of human visual motion perception. *Vision Research, 35,* 2697–2722. [PubMed]

Lu, Z. L., & Sperling, G. (2001). Three-systems theory of human visual motion perception: Review and update. *Journal of the Optical Society of America A, Optics, Image Science, and Vision, 18,* 2331–2370. [PubMed]

MacLeod, D. I., Williams, D. R., & Makous, W. (1992). A visual nonlinearity fed by single cones. *Vision Research, 32,* 347–363. [PubMed]

Pelli, D. G. (1981). *The effects of visual noise*. Cambridge: Cambridge University.

Pelli, D. G. (1990). The quantum efficiency of vision. In C. Blakemore (Ed.), *Visual coding and efficiency* (pp. 3–24). Cambridge: Cambridge University Press.

Pelli, D. G., & Farell, B. (1999). Why use noise? *Journal of the Optical Society of America A, Optics, Image Science, and Vision, 16,* 647–653. [PubMed]

Ross, J., & Speed, H. D. (1996). Perceived contrast following adaptation to gratings of different orientations. *Vision Research, 36,* 1811–1818. [PubMed]

Schofield, A. J., & Georgeson, M. A. (1999). Sensitivity to modulations of luminance and contrast in visual white noise: Separate mechanisms with similar behaviour. *Vision Research, 39,* 2697–2716. [PubMed]

Schofield, A. J., & Georgeson, M. A. (2000). The temporal properties of first- and second-order vision. *Vision Research, 40,* 2475–2487. [PubMed]

Scott-Samuel, N. E., & Georgeson, M. A. (1999). Does early non-linearity account for second-order motion? *Vision Research, 39,* 2853–2865. [PubMed]

Seiffert, A. E., & Cavanagh, P. (1999). Position-based motion perception for color and texture stimuli: Effects of contrast and speed. *Vision Research, 39,* 4172–4185. [PubMed]

Smith, A. T., & Ledgeway, T. (1997). Separate detection of moving luminance and contrast modulations: Fact or artifact? *Vision Research, 37,* 45–62. [PubMed]

Snowden, R. J., & Hammett, S. T. (1992). Subtractive and divisive adaptation in the human visual system. *Nature, 355,* 248–250. [PubMed]

Snowden, R. J., & Hammett, S. T. (1996). Spatial frequency adaptation: Threshold elevation and perceived contrast. *Vision Research, 36,* 1797–1809. [PubMed]

Taub, E., Victor, J. D., & Conte, M. M. (1997). Nonlinear preprocessing in short-range motion. *Vision Research, 37,* 1459–1477. [PubMed]

Ukkonen, O. I., & Derrington, A. M. (2000). Motion of contrast-modulated gratings is analysed by different mechanisms at low and at high contrasts. *Vision Research, 40,* 3359–3371. [PubMed]

Wilson, H. R., Ferrera, V. P., & Yo, C. (1992). A psychophysically motivated model for two-dimensional motion perception. *Visual Neuroscience, 9,* 79–97. [PubMed]

Zaidi, Q., & DeBonet, J. S. (2000). Motion energy versus position tracking: Spatial, temporal, and chromatic parameters. *Vision Research, 40,* 3613–3635. [PubMed]